

Stochastic Galerkin Projection and Numerical Integration for Stochastic Systems of Equations

Markus Wahlsten^a, Jan Nordström^b

^a*Department of Mathematics, Computational Mathematics, Linköping University,
SE-581 83 Linköping, Sweden (markus.wahlsten@liu.se).*

^b*Department of Mathematics, Computational Mathematics, Linköping University,
SE-581 83 Linköping, Sweden (jan.nordstrom@liu.se).*

Abstract

An incompletely parabolic system in three space dimensions with stochastic boundary and initial data is studied. The intrusive approach where we combine polynomial chaos with stochastic Galerkin projection is compared to the non-intrusive approach, where quadrature rules in combination with probability density functions of the prescribed uncertainties are used. The two methods are compared when calculating statistics for the compressible Navier–Stokes equations. As a measure of comparison, variance size, computational efficiency and accuracy are used.

Keywords: uncertainty quantification, stochastic data, polynomial chaos, stochastic Galerkin, intrusive methods, non-intrusive methods, Navier–Stokes equations.

1. Introduction

There are essentially two different methods for uncertainty quantification related to initial boundary value problems. Non-intrusive methods solve the original deterministic problem using a particular stochastic input. Standard quadrature techniques, often combined with sparse grid techniques can be used to obtain the statistics of interest. Intrusive methods are based on polynomial chaos (PC) expansions leading to a system of equations for the expansion coefficients. In contrast to the non-intrusive case, a new non-deterministic code must be developed.

The focus in this paper will be on the comparison in performance between numerical integration (NI) and PC with stochastic Galerkin (SG) approach.

Preprint submitted to Journal of Computational Physics

March 8, 2017

The comparison is performed using the variance reducing boundary conditions derived in [1] and [2] for the compressible Navier–Stokes equations.

The rest of the paper proceeds as follows. In Section 2 a general continuous incompletely parabolic system of equations is introduced. Next, in Section 3, the PC-SG procedure is presented and the system of equations for the expansion coefficients is derived. The non-intrusive approach using NI is described in Section 4. Section 5 introduces a stable and accurate semi-discrete finite difference formulation of the two continuous problems. Further, the technique is applied to the compressible Navier–Stokes equations in Section 6 and a comparison of NI and PC-SG is done. Finally, conclusions are drawn in Section 7.

2. The continuous problem

Consider the following system of equations with stochastic boundary and initial data,

$$\begin{aligned} u_t + Au_x + Bu_y + Cu_z &= F_x(u) + G_y(u) + H_z(u), & \vec{x} \in \Omega, & \quad t > 0, \\ Lu &= g(\vec{x}, t, \vec{\xi}), & \vec{x} \in \partial\Omega, & \quad t > 0, \\ u &= f(\vec{x}, \vec{\xi}), & \vec{x} \in \Omega, & \quad t = 0, \end{aligned} \tag{1}$$

where,

$$\begin{aligned} F(u) &= D_{11}u_x + D_{12}u_y + D_{13}u_z, \\ G(u) &= D_{21}u_x + D_{22}u_y + D_{23}u_z, \\ H(u) &= D_{31}u_x + D_{32}u_y + D_{33}u_z. \end{aligned} \tag{2}$$

We denote the solution by the vector $u = u(\vec{x}, t, \vec{\xi}) = [u^{(1)}, \dots, u^{(N)}]$, where, $\vec{x} = (x, y, z)$, and $\vec{\xi} = (\xi_1, \xi_2, \dots, \xi_L)$ is the vector of variables representing the uncertainty in the solution. The $N \times N$ matrices A, B, C, D_{ij} are constant and symmetric. The matrices D_{ij} , $i, j = 1, 2, 3$ are singular, leading to an incompletely parabolic problem. L is the boundary operator defined on $\partial\Omega$, while $f(\vec{x}, \vec{\xi})$ and $g(\vec{x}, t, \vec{\xi})$ are the stochastic initial and boundary data.

The boundary operator can be written on the general form

$$L = L^- - RL^+ \tag{3}$$

with a certain restriction on the matrix R . With a slight abuse of notation we denote L^+u and L^-u , the outgoing and ingoing generalized characteristic variables respectively. See [2, 3] for a complete derivation of L^+ and L^- and conditions on the matrix R leading to well-posedness.

3. Polynomial chaos expansion with stochastic Galerkin projection

The polynomial chaos framework considered in this paper is based on expansions of polynomials introduced by Ghanem and Spanos [4] and later generalized by Xiu and Karniadakis [5].

3.1. Polynomial chaos

Let $(\Omega_\xi, \mathcal{A}, \mathcal{P})$ be the probability space, where Ω_ξ is the event space, \mathcal{A} the σ -field of subsets of Ω_ξ , and \mathcal{P} the probability measure [6]. Consider a general orthogonal chaos basis $\{\psi_i(\xi)\}_{i=0}^\infty$, satisfying

$$\langle \psi_i, \psi_j \rangle = \int_{\Omega_\xi} \psi_i(\xi) \psi_j(\xi) d\mathcal{P}(\xi) = \delta_{ij}. \quad (4)$$

A *second order* random field $u(x, t, \xi)$ satisfying $\int_{\Omega_\xi} u(x, t, \xi)^2 d\mathcal{P}(\xi) < \infty$, can be written as

$$u(x, t, \xi) = \sum_{k=0}^{\infty} u_k(x, t) \psi_k(\xi) \quad (5)$$

where the coefficients $\{u_k(x, t)\}_{k=0}^\infty$ are given by the projections

$$u_k(x, t) = \langle u(x, t, \xi), \psi_k(\xi) \rangle, \quad k = 0, 1, \dots \quad (6)$$

The mean and variance can be expressed as

$$\mathbb{E}[u] = \int_{\Omega_\xi} u d\mathcal{P}(\xi) = u_0, \quad (7)$$

and

$$\text{Var}[u] = \mathbb{E}[u^2] - \mathbb{E}[u]^2 = \int_{\Omega_\xi} \sum_{k=0}^{\infty} u_k^2 \psi_k^2 d\mathcal{P}(\xi) - u_0^2 = \sum_{k=1}^{\infty} u_k^2 \quad (8)$$

which follows from the orthogonality property of the basis functions $\{\psi_i\}_{i=0}^\infty$. For more details on the polynomial chaos technique, see [7].

3.2. The stochastic Galerkin projection

Next, in order to approximately compute the various statistics of the solution to the problem, we insert the truncated expansion

$$u(\vec{x}, t, \vec{\xi}) = \sum_{k=0}^M u_k(\vec{x}, t) \psi_k(\vec{\xi}), \quad (9)$$

into (1), to get

$$\begin{aligned}
\sum_{k=0}^M (u_k)_t \psi_k &+ \sum_{k=0}^M A(u_k)_x \psi_k + \sum_{k=0}^M B(u_k)_y \psi_k + \sum_{k=0}^M C(u_k)_z \psi_k \\
&= \sum_{k=0}^M F_x(u_k \psi_k) + \sum_{k=0}^M G_y(u_k \psi_k) + \sum_{k=0}^M H_z(u_k \psi_k), \\
\sum_{k=0}^M L u_k \psi_k &= g(\vec{x}, t, \vec{\xi}), \\
\sum_{k=0}^M u_k \psi_k &= f(\vec{x}, \vec{\xi}).
\end{aligned} \tag{10}$$

Next, we perform a Galerkin projection, that is, we multiply (10) by ψ_l , for $l = 0, 1, \dots, M$ and integrate over the stochastic domain Ω , to obtain

$$\begin{aligned}
\int_{\Omega} \sum_{k=0}^M (u_k)_t \psi_k \psi_l d\mathcal{P} &+ \int_{\Omega} \sum_{k=0}^M [A(u_k)_x \psi_k \psi_l + B(u_k)_y \psi_k \psi_l \\
&+ C(u_k)_z \psi_k \psi_l] d\mathcal{P} \\
&= \int_{\Omega} \sum_{k=0}^M [F_x(u_k \psi_k \psi_l) + G_y(u_k \psi_k \psi_l) \\
&+ H_z(u_k \psi_k \psi_l)] d\mathcal{P}, \\
\int_{\Omega} \sum_{k=0}^M L u_k \psi_k \psi_l d\mathcal{P} &= \int_{\Omega} g(\vec{x}, t, \vec{\xi}) \psi_l d\mathcal{P}, \\
\int_{\Omega} \sum_{k=0}^M u_k \psi_k \psi_l d\mathcal{P} &= \int_{\Omega} f(\vec{x}, \vec{\xi}) \psi_l d\mathcal{P}, \quad \text{for } l = 0, 1, \dots, M,
\end{aligned} \tag{11}$$

which in compact notation can be written

$$\begin{aligned}
\sum_{k=0}^M (u_k)_t \langle \psi_k, \psi_l \rangle &+ \sum_{k=0}^M [A(u_k)_x + B(u_k)_y + C(u_k)_z] \langle \psi_k, \psi_l \rangle \\
&= \sum_{k=0}^M [F_x(u_k) + G_y(u_k) + H_z(u_k)] \langle \psi_k, \psi_l \rangle, \\
\sum_{k=0}^M Lu_k \langle \psi_k, \psi_l \rangle &= \langle g(\vec{x}, t, \vec{\xi}), \psi_l \rangle, \\
\sum_{k=0}^M Lu_k \langle \psi_k, \psi_l \rangle &= \langle f(\vec{x}, \vec{\xi}), \psi_l \rangle, \quad \text{for } l = 0, 1, \dots, M.
\end{aligned} \tag{12}$$

From the orthogonality property (4), (12) reduces to

$$\begin{aligned}
(u_l)_t + A(u_l)_x + B(u_l)_y + C(u_l)_z &= F_x(u_l) + G_y(u_l) + H_z(u_l) \\
Lu_l &= \langle g(\vec{x}, t, \vec{\xi}), \psi_l \rangle \\
u_l &= \langle f(\vec{x}, \vec{\xi}), \psi_l \rangle
\end{aligned} \tag{13}$$

for $l = 0, 1, \dots, M$. Hence, a deterministic system of dimension $M + 1$ times the original system is obtained. From (13), the deterministic coefficients $u_0(\vec{x}, t), u_1(\vec{x}, t), \dots, u_M(\vec{x}, t)$ are computed.

4. Numerical integration

The most commonly used non-intrusive technique, the Monte Carlo method [8], will not be considered here. The method is advantageous for large number of stochastic dimensions, but not competitive for low to moderate number of uncertainties. In this paper we consider numerical integration based on quadrature techniques.

Integration and quadrature relations in one dimension can be written

$$\int_a^b f(q) \rho(q) dq \approx \sum_{m=1}^M f(q^m) w^m \tag{14}$$

where f is the function we want to integrate and ρ is the corresponding density function. We denote M as the number of grid points, q^m and w^m as the quadrature points in probabilistic space and the corresponding weights respectively. The choice of quadrature points and weights determines the

accuracy of the method. For simplicity, we will use Simpson's rule [9] as the integration technique in this paper.

The NI method can easily be extended to several dimensions, that is

$$\int_{\Gamma} f(\tilde{q}) \rho(\tilde{q}) d\tilde{q} \approx \sum_{m_1=1}^{M_1} \cdots \sum_{m_p=1}^{M_p} f(q_1^{m_1}, \dots, q_p^{m_p}) w^{m_1} \cdots w^{m_p}, \quad (15)$$

where Γ is the p -dimensional domain and $\tilde{q} = (q_1, \dots, q_p)$. The q^m 's and w^r 's correspond to the points and weights of their respective quadrature rule.

5. The semi-discrete formulation

Despite the fact that uncertainties are present in our model, the final problem formulation that arises from the stochastic Galerkin projection is strictly deterministic. We will solve (13) using a semi-discrete finite difference formulation based on the SBP–SAT technique [10, 11, 12, 13]. The reader is referred to [2, 3] for complete technical details.

A stable and accurate semi-discrete formulation of (13) on SBP–SAT form can be expressed as,

$$\begin{aligned} v_t &+ (I_M \otimes D_x \otimes I_y \otimes I_z \otimes A)v + (I_M \otimes I_x \otimes D_y \otimes I_z \otimes B)v \\ &+ (I_M \otimes I_x \otimes I_y \otimes D_z \otimes C)v \\ &= (I_M \otimes D_x \otimes I_y \otimes I_z \otimes I_N)F + (I_M \otimes I_x \otimes D_y \otimes I_z \otimes I_N)G \\ &+ (I_M \otimes I_x \otimes I_y \otimes D_z \otimes I_N)H \\ &+ (I_M \otimes P_x^{-1} E_{N_x} \otimes I_y \otimes I_z \otimes I_N)(\tilde{\Sigma}(\tilde{L}^- - \tilde{R}\tilde{L}^+)v - \tilde{g} \otimes e_{N_x}) \\ v(0) &= \tilde{f}. \end{aligned} \quad (16)$$

In (16), v represent u numerically, \tilde{g} and \tilde{f} are the numerical approximations of $\langle g(\vec{x}, t, \vec{\xi}), \psi_l \rangle$, and $\langle f(\vec{x}, t, \vec{\xi}), \psi_l \rangle$ for $l = 0, 1, \dots, M$ respectively. To ease the notation, we only consider the boundary at $x = 1$. The treatment of the remaining boundaries is completely analogous. Note that the complete system (16) computes all coefficients and evaluations in ξ for PC-SG and NI respectively.

Remark 1. *The semi-discrete formulation is similar when computing the solution using NI. The differences will be pointed out below by formal remarks.*

The numerical solution is arranged in the following way

$$\begin{aligned}
v &= \begin{bmatrix} v_0 \\ v_1 \\ \vdots \\ [v_m] \\ \vdots \\ v_M \end{bmatrix}, & [v_m] &= \begin{bmatrix} v_0 \\ v_1 \\ \vdots \\ [v_i] \\ \vdots \\ v_{N_x} \end{bmatrix}_m, & [v_i]_m &= \begin{bmatrix} v_0 \\ v_1 \\ \vdots \\ [v_j] \\ \vdots \\ v_{N_y} \end{bmatrix}_{mi}, \\
[v_j]_{mi} &= \begin{bmatrix} v_0 \\ v_1 \\ \vdots \\ [v_k] \\ \vdots \\ v_{N_z} \end{bmatrix}_{mij}, & [v_n]_{mij} &= \begin{bmatrix} v_0 \\ v_1 \\ \vdots \\ [v_n] \\ \vdots \\ v_M \end{bmatrix}_{mijk},
\end{aligned}$$

where v_{mijkn} approximates the polynomial chaos coefficient $u_m^{(n)}(x_i, y_j, z_k, t)$.

Remark 2. The vector v_{mijkn} approximates $u^{(n)}(x_i, y_j, z_k, t, \xi_m)$ when computing the solution using NI.

The first derivative in the x , y and z direction is approximated by $D_{x,y,z} = P_{x,y,z}^{-1} Q_{x,y,z}$, respectively. The matrices $P_{x,y,z}$ are positive definite diagonal matrices and $Q_{x,y,z}$ are almost skew-symmetric matrices satisfying $Q_{x,y,z} + Q_{x,y,z}^T = E_{N_{x,y,z}} - E_{0_{x,y,z}} = \mathbb{B} = \text{diag}[-1, 0, \dots, 0, 1]$. Further, we denote I_x , I_y , I_z , I_N and I_M as identity matrices of dimension $N_x + 1$, $N_y + 1$, $N_z + 1$, N and $M + 1$. The matrices E_{0_x} and E_{N_x} are zero except for the element $(1, 1)$ and $(N_x + 1, N_x + 1)$ respectively, which is 1. Moreover, the vector e_{N_x} is a zero vector with the exception of the last element which is 1.

The numerical fluxes in (16) are given by

$$\begin{aligned}
F &= (I_M \otimes \tilde{I} \otimes D_{11})v_x + (I_M \otimes \tilde{I} \otimes D_{12})v_y + (I_M \otimes \tilde{I} \otimes D_{13})v_z, \\
G &= (I_M \otimes \tilde{I} \otimes D_{21})v_x + (I_M \otimes \tilde{I} \otimes D_{22})v_y + (I_M \otimes \tilde{I} \otimes D_{23})v_z, \\
H &= (I_M \otimes \tilde{I} \otimes D_{31})v_x + (I_M \otimes \tilde{I} \otimes D_{32})v_y + (I_M \otimes \tilde{I} \otimes D_{33})v_z,
\end{aligned} \tag{17}$$

together with the notation $\tilde{I} = (I_x \otimes I_y \otimes I_z)$ and the abbreviations

$$\begin{aligned}
v_x &= (I_M \otimes D_x \otimes I_y \otimes I_z \otimes I_N)v, \\
v_y &= (I_M \otimes I_x \otimes D_y \otimes I_z \otimes I_N)v, \\
v_z &= (I_M \otimes I_x \otimes I_y \otimes D_z \otimes I_N)v.
\end{aligned} \tag{18}$$

The boundary and initial data \tilde{g} and \tilde{f} , are the projections

$$\tilde{g} = \begin{bmatrix} \langle \bar{g}(\xi), \psi_0(\xi) \rangle \\ \langle \bar{g}(\xi), \psi_1(\xi) \rangle \\ \vdots \\ \langle \bar{g}(\xi), \psi_M(\xi) \rangle \end{bmatrix}, \quad \tilde{f} = \begin{bmatrix} \langle \bar{f}(\xi), \psi_0(\xi) \rangle \\ \langle \bar{f}(\xi), \psi_1(\xi) \rangle \\ \vdots \\ \langle \bar{f}(\xi), \psi_M(\xi) \rangle \end{bmatrix}. \quad (19)$$

In (19), we denote $\bar{g}(\xi)$ and $\bar{f}(\xi)$ as the original boundary and initial data vector as a function of ξ injected on all grid points at the plane $x = 1$ and $t = 0$ respectively. The inner products $\langle \bar{g}(\xi), \psi_m(\xi) \rangle$ and $\langle \bar{f}(\xi), \psi_m(\xi) \rangle$ are computed numerically using NI.

Remark 3. When computing the solution using NI, the vectors \tilde{g} and \tilde{f} instead denote $\tilde{g} = [\bar{g}(\xi_0), \bar{g}(\xi_1), \dots, \bar{g}(\xi_M)]^T$ and $\tilde{f} = [\bar{f}(\xi_0), \bar{f}(\xi_1), \dots, \bar{f}(\xi_M)]^T$. Hence, the boundary and initial data $\bar{g}(\xi)$ and $\bar{f}(\xi)$ are discretized in ξ .

The discrete boundary operators \tilde{L}^+ and \tilde{L}^- are decomposed as

$$\begin{aligned} \tilde{L}^+ &= (I_M \otimes I_x \otimes I_y \otimes I_z \otimes L_0^+) + (I_M \otimes D_x \otimes I_y \otimes I_z \otimes L_{D_x}^+) \\ &\quad + (I_M \otimes I_x \otimes D_y \otimes I_z \otimes L_{D_y}^+) + (I_M \otimes I_x \otimes I_y \otimes D_z \otimes L_{D_z}^+) \\ \tilde{L}^- &= (I_M \otimes I_x \otimes I_y \otimes I_z \otimes L_0^-) + (I_M \otimes D_x \otimes I_y \otimes I_z \otimes L_{D_x}^-) \\ &\quad + (I_M \otimes I_x \otimes D_y \otimes I_z \otimes L_{D_y}^-) + (I_M \otimes I_x \otimes I_y \otimes D_z \otimes L_{D_z}^-). \end{aligned} \quad (20)$$

In (20), the matrices L_0^+ , L_0^- , $L_{D_x}^+$, $L_{D_x}^-$, $L_{D_y}^+$, $L_{D_y}^-$, $L_{D_z}^+$, and $L_{D_z}^-$ correspond to the continuous boundary operators, see [2, 3] for a complete description. In a similar fashion, the matrix \tilde{R} is defined as

$$\tilde{R} = (\tilde{I} \otimes R \otimes I_M). \quad (21)$$

where R is the matrix corresponding to the continuous boundary conditions (3). The penalty matrix $\tilde{\Sigma}$ is chosen such that stability is achieved. Again, for a complete derivation and proof of stability for the semi-discrete formulation, the reader is referred to [2, 3]

6. An example

To exemplify the difference between NI and PC-SG, we consider the linearized symmetrized Navier–Stokes equations in one dimension [14],

$$U_t + AU_x = \epsilon BU_{xx}, \quad 0 < x < 1, \quad t > 0, \quad (22)$$

where

$$B = \text{diag} \left(0, \frac{\lambda + 2\mu}{\bar{\rho}}, \frac{\gamma\mu}{\text{Pr}\bar{\rho}} \right). \quad (23)$$

We also use $A = X\Lambda X^T$, where

$$\Lambda = \begin{bmatrix} \bar{u} & 0 & 0 \\ 0 & \bar{u} + \bar{c} & 0 \\ 0 & 0 & \bar{u} - \bar{c} \end{bmatrix}, \quad X = \begin{bmatrix} -\sqrt{\frac{\gamma-1}{\gamma}} & \frac{1}{\sqrt{2\gamma}} & \frac{1}{\sqrt{2\gamma}} \\ 0 & \frac{1}{\sqrt{2\gamma}} & -\frac{1}{\sqrt{2\gamma}} \\ \frac{1}{\sqrt{\gamma}} & \sqrt{\frac{\gamma-1}{2\gamma}} & \sqrt{\frac{\gamma-1}{2\gamma}} \end{bmatrix}. \quad (24)$$

The parameters in (22), (23) and (24) are μ , λ , Pr , ϵ and represent the dynamic and second viscosity, the Prandtl number and the inverse Reynolds number. In the calculations we use the following parameters

$$\begin{aligned} \bar{\rho} &= 1, & \bar{u} &= 1, & \bar{c} &= 2, & \bar{p} &= 1, & \lambda &= -2/3, \\ \gamma &= 1.4, & \epsilon &= 0.01, & \text{Pr} &= 0.7, & \mu &= 1. \end{aligned} \quad (25)$$

The boundary conditions are of the form (3), where the matrices R_0 and R_1 are of sizes 3×2 and 2×3 defined on the boundaries $x = 0$ and $x = 1$ respectively. For simplicity, we use zero matrices for R_0 and R_1 .

Randomness is imposed in the initial and boundary data given by the manufactured solutions

$$\begin{aligned} \rho_1 &= u_1 = p_1 = \sin(2\pi(x-t)) + \xi \sin(\xi/2 - t) \cos(x - \xi), \\ \rho_2 &= u_2 = p_2 = \sin(2\pi(x-t)) + \sin(5(\xi/2 - t)) \cos(2(x - 5\xi)), \end{aligned} \quad (26)$$

with the additional forcing function

$$F = W_t + AW_x - \epsilon BW_{xx}, \quad W = [\rho_{1,2}, u_{1,2}, p_{1,2}]^T. \quad (27)$$

We have chosen the manufactured solutions with subscript 1 and 2 in (26) to illustrate the effects of smoothness. The solution with subscript 1 is considered to be smooth, while 2 is considered to be less smooth. The resulting system is then

$$\begin{aligned} U_t + AU_x &= \epsilon BU_{xx} + F, & 0 < x < 1, & t > 0, \\ L_0 U &= L_0 W & x = 0 & t > 0 \\ L_1 U &= L_1 W & x = 1 & t > 0 \\ U &= W & 0 < x < 1 & t = 0 \end{aligned} \quad (28)$$

The normed error of the variance that is used for comparison is given by

$$\|\text{Var}[e]\| = \int_0^T \|\text{Var}[U] - \text{Var}[W]\|_2 dt. \quad (29)$$

In the calculations, we use 3rd-order SBP-operators with 40 grid points in space together with the 4th-order Runge-Kutta scheme as time integrator. To minimize the effects of the deterministic errors we use a PC-SG computation with 30 basis functions instead of an exact solution as reference solution. The uncertainty ξ is uniformly distributed between -1 and 1 .

Figure 1 and 2 show the normed error of the variance as a function of number of evaluations (M) for PC-SG and NI using different manufactured solutions. Note that NI requires at least three points, hence it does not overlap with PC-SG. As can be seen, the rate of convergence is significantly higher for the PC-SG method than for NI. The rate of convergence for the NI (Simpson's rule) is in line with theory, that is 4th order. Also, we note that the PC-SG requires more evaluations to perform better than NI.

Figure 3 and 4 illustrate how the total CPU time is affected by the number of evaluations for both methods. Finally, Figure 5 and 6 present the normed error of the variance as a function of CPU time. For a small number of evaluations, the results indicate a better performance for NI, however for moderate and large number of evaluations PC-SG performs significantly better.

7. Conclusions

A comparison between the intrusive PC-SG and non-intrusive NI have been presented. The study has been carried out on a general incompletely parabolic system of equations. The PC-SG procedure was applied to the continuous problem and a provably stable numerical formulation based on SBP-SAT was constructed. Due to linearity, the numerical scheme for the PC-SG and NI differs only for the initial and boundary data treatments.

The linearized Navier–Stokes equations using generalized characteristic boundary conditions are considered when comparing the two methods. As comparison, the normed error of the variance was used. The numerical results indicate that the PC-SG outperforms NI for the problems considered. Although the cost is higher for the PC-SG, the convergence is faster. The effects are significant for larger number of realizations. We conclude that

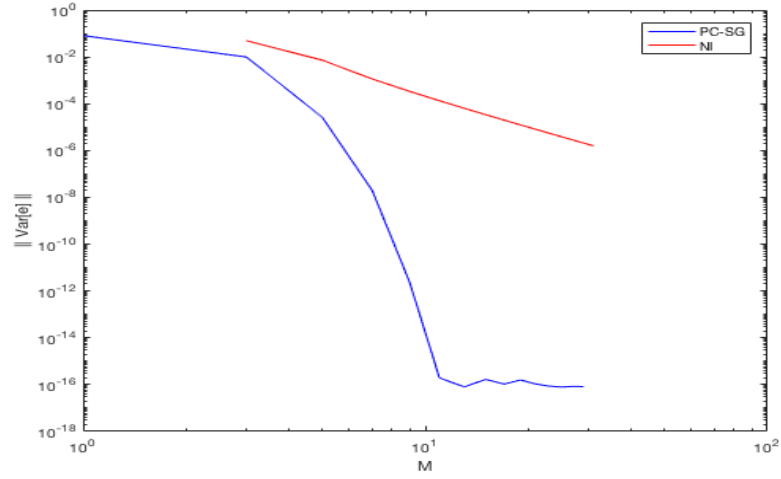


Figure 1: The normed error of the variance as a function of M for a uniformly distributed ξ for the methods NI and PC-SG, using a smooth manufactured solution.

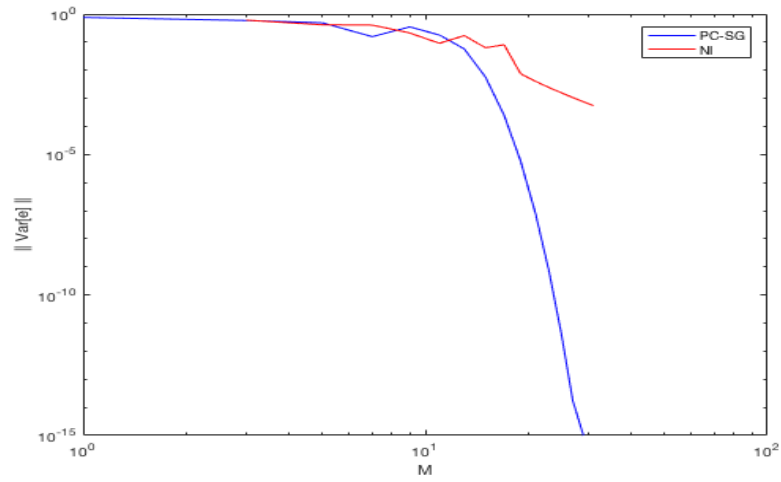


Figure 2: The normed error of the variance as a function of M for a uniformly distributed ξ for the methods NI and PC-SG, using a less smooth manufactured solution.

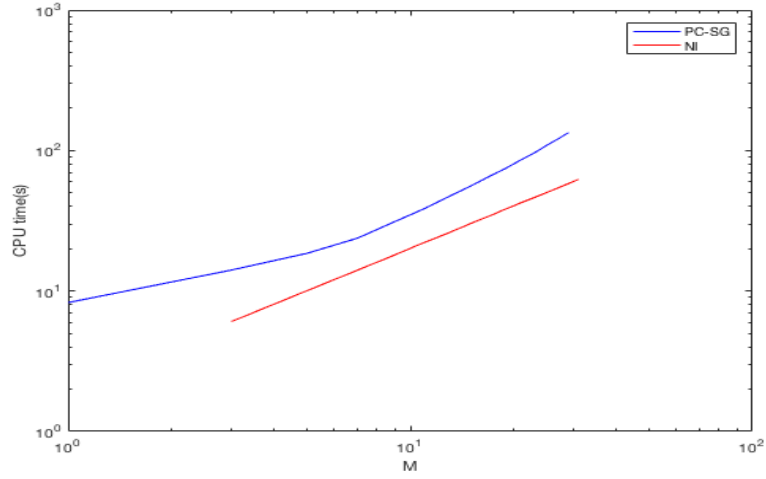


Figure 3: The total computation time as a function of M for a uniformly distributed ξ for the methods NI and PC-SG, using a smooth manufactured solution.

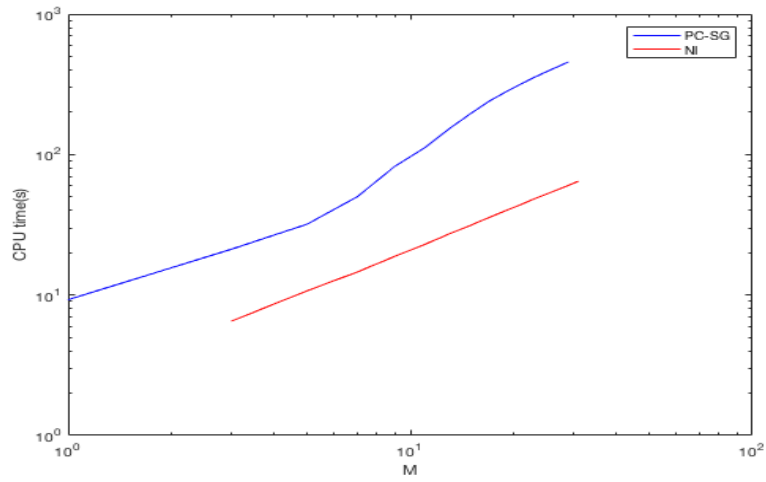


Figure 4: The total computation time as a function of M for a uniformly distributed ξ for the methods NI and PC-SG, using a less smooth manufactured solution.

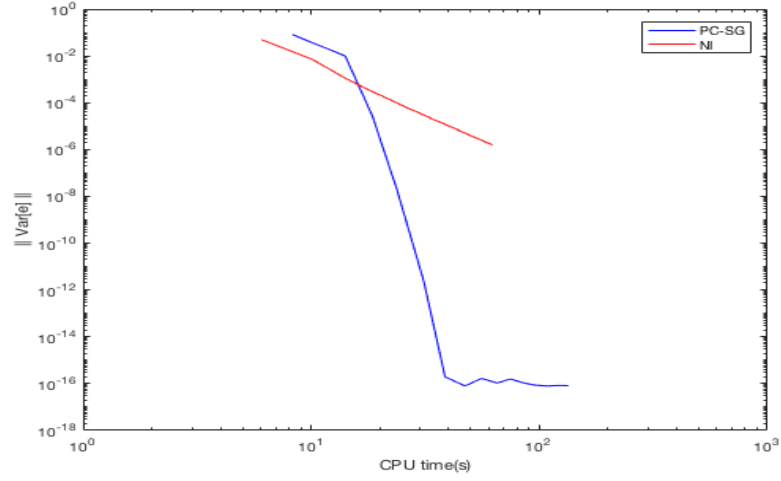


Figure 5: The normed error of the variance as a function of computation time for a uniformly distributed ξ for the methods NI and PC-SG, using a smooth manufactured solution.

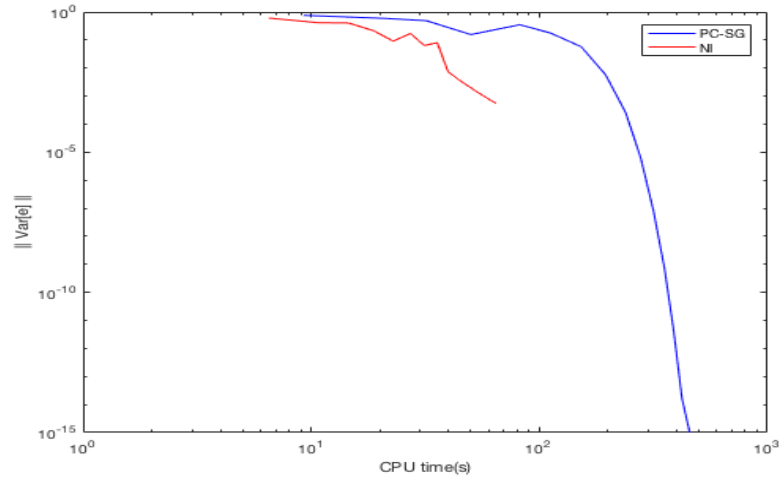


Figure 6: The normed error of the variance as a function of computation time for a uniformly distributed ξ for the methods NI and PC-SG, using a less smooth manufactured solution.

the reduced performance for less smooth problems is more pronounced for PC-SG compared to NI.

References

- [1] J. Nordström, M. Wahlsten, Variance reduction through robust design of boundary conditions for stochastic hyperbolic systems of equations, *J COMPUT PHYS* 282 (2015) 1–22.
- [2] M. Wahlsten, J. Nordström, Robust Boundary Conditions for Stochastic Incompletely Parabolic Systems of Equations, In production (2016).
- [3] J. Nordström, A Roadmap to Well Posed and Stable Problems in Computational Physics, Accepted in *J SCI COMPUT* (2016).
- [4] R. Ghanem, S. Dham, Stochastic finite element analysis for multiphase flow in heterogeneous porous media, *TRANSPORT POROUS MED* 32 (1998) 239–262.
- [5] D. Xiu, G. E. Karniadakis, The Wiener–Askey polynomial chaos for stochastic differential equations, *SIAM journal on scientific computing* 24 (2002) 619–644.
- [6] W. Feller, An introduction to probability theory and its applications: volume I, volume 3, John Wiley & Sons London-New York-Sydney-Toronto, 1968.
- [7] M. P. Pettersson, G. Iaccarino, J. Nordstrom, Polynomial chaos methods for hyperbolic partial differential equations, *Springer Math Eng.* doi 10 (2015) 978–3.
- [8] J. Hammersley, Monte carlo methods, Springer Science & Business Media, 2013.
- [9] P. J. Davis, P. Rabinowitz, Methods of numerical integration, Courier Corporation, 2007.
- [10] B. Strand, Summation by parts for finite difference approximations for d/dx , *J COMPUT PHYS* 110 (1994) 47–67.

- [11] M. Svärd, J. Nordström, On the order of accuracy for difference approximations of initial-boundary value problems, J COMPUT PHYS 218 (2006) 333–352.
- [12] K. Mattsson, J. Nordström, Summation by parts operators for finite difference approximations of second derivatives, J COMPUT PHYS 199 (2004) 503–540.
- [13] J. Nordström, M. H. Carpenter, Boundary and interface conditions for high order finite difference methods applied to the Euler and Navier-Stokes equations, J COMPUT PHYS 148 (1999) 621–645.
- [14] J. Nordström, The use of characteristic boundary conditions for the Navier-Stokes equations, COMPUT FLUIDS 24 (1995) 609–623.